ANALYSIS FOR MAGNETIC AND RADIATION SPECTRAL PROPERTIES OF UNDULATORS AT HISOR

A. Hiraya, N. V. Smolyakov[#], H. Yoshida, HSRC & Hiroshima University
T. Muneyoshi, G. Rybalchenko, K. Shirasawa, Hiroshima University
D. Amano, T. Takayama, Sumitomo Heavy Industries, Ltd.

Abstract

A compact, racetrack type storage ring HiSOR has been constructed at Hiroshima Synchrotron Radiation Center. A linear undulator and a new type of helical/linear undulator were installed at the two straight sections of HiSOR. Their magnetic fields were measured for different configurations and gaps. The analysis of experimentally measured magnetic field data and radiation spectra are made for HiSOR undulators and presented in this report.

1 INTRODUCTION

HiSOR racetrack type storage ring [1] is planned for SR research on science and technology using VUV to X-ray up to 5 keV. It has two straight sections with the length 8240 mm. The stored electron beam energy is 700 MeV, the current is 300 mA bending magnetic field is 2.7 T, synchrotron radiation critical energy is 880 eV. Electron beam has the following parameters at the center of straight sections: horizontal size is 1.51 mm, vertical size is 0.126 mm, horizontal divergence is 0.412 mrad, vertical divergence is 0.063 mrad at 0.02 emittance coupling. Two undulators are already installed at HiSOR storage ring [2].

This paper studies the influence of magnetic field errors on the performance of helical/linear undulator. Various studies of such kind effect have been carried out in a number of paper [3-11]. In the first papers [3-6] the quality of the wiggler field was characterised by its RMS peak magnetic field error. However, as it has been shown in [7], this deviation is not strongly correlated with the observed reduction in radiation peak intensity; instead, the radiation intensity is well correlated with the RMS phase error [7-9]. But the most straightforward way to estimate theoretically the performance of undulator is to calculate its radiation characteristics with the use of experimentally measured magnetic field. Such approach was used in a number of papers [6, 10, 11], and have been successfully applied in this study. The new effective, universal and fast computer code was created to calculate the variety of undulator radiation characteristics. Suffice it to say that it needs only 130 seconds to calculate radiation distribution in real geometry (90*90=8100 points on the screen, measured magnetic field with its length = 2.5 meters, real electron beam emittance) at PC Pentium II, 333 MHz.

[#] Email: nick@sci.hiroshima-u.ac.jp

2 PARAMETERS OF UNDULATORS

The linear undulator has a standard pure-permanent magnet design with eight magnetic blocks per period (including upper and lower jaws) and will generate the radiation with 25-300 eV photon energy. The helical/ linear undulator consists of upper and lower jaws same as standard planar undulator while each jaw consists of one fixed magnet array at the center and two magnet arrays at both sides. By longitudinal shift of side magnet arrays, the amplitudes of vertical and horizontal magnetic fields can be varied. In this way the proper polarization of radiation, generated by this undulator, can be selected as linear, elliptical, right- or left-circular. It gives almost perfect circular polarized light in 4 - 40 eV region in the helical configuration, as well as linear polarized light in 3 - 300 eV in the linear configuration. The main parameters of the undulators (with computed magnetic field amplitudes) are shown in Tables 1 and 2.

Table 1: Parameters of linear undulator

Period length	57 mm
Number of periods	41
Total length	2354.2 mm
Gap distance	30 - 200 mm
Permanent magnet	NdFeB
Maximum magnetic field	0.41 T
Deflection parameter	2.2

Table 2: Parameters of helical/linear undulator

Period length	100 mm
Number of periods	18
Total length	1828.6 mm
Gap distance	30 - 200 mm
Permanent magnet	NdFeB
Max. magnetic field (helical mode)	0.347 T
Deflection parameter (helical mode)	4.6
Max. magnetic field (linear mode)	0.597 T
Deflection parameter (linear mode)	5.6

Calculated photon flux densities at helical and linear modes of the helical/linear undulator, those of the linear undulator (with sinusoidal magnetic fields) and the bending magnet at HiSOR are shown in Fig. 1.

0-7803-5573-3/99/$10.00@1999 IEEE.

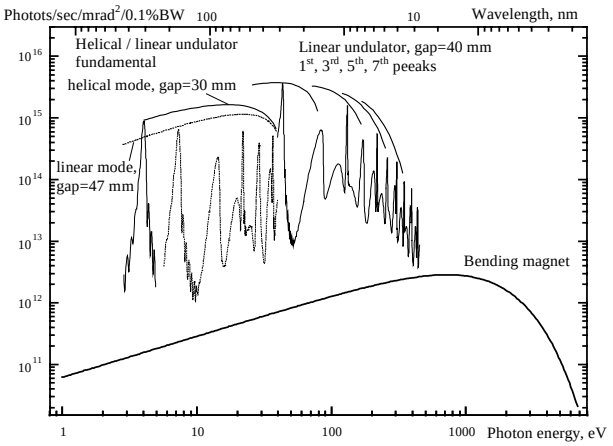

Fig.1. Calculated flux density distributions of two undulators and bending magnet at HiSOR.

3 PERFORMANCE OF HELICAL/ LINEAR UNDULATOR

3.1 Helical mode

The measured horizontal and vertical components of the undulator's magnetic field are shown in Fig. 2.

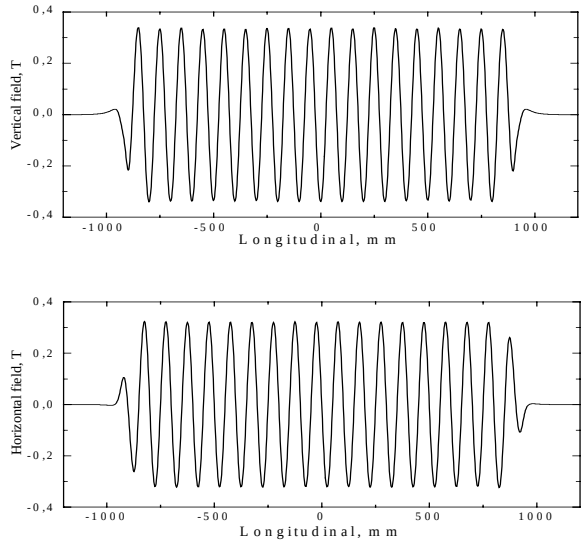

Fig. 2. Measured magnetic fields of helical/linear undulator at helical mode, gap=30 mm.

The analysis show that the horizontal B_x and vertical B_y fields can be fitted by the formula:

$$B_{x,y} = C_{x,y} + A_{x,y}\sin(2\pi z\,{}^{z}\!/\!_{\lambda_w} + \varphi_{x,y})$$

where C_x = -2.5 Gs, A_x = 3228 Gs, $\varphi_x = 0$, C_y = -7.1 Gs, A_y = 3397 Gs, $\varphi_y = 1.6$, λ_w = 100 mm.

The computed horizontal and vertical trajectories of the electron in the measured field with steering magnets orbit adjustment are shown in Fig. 3. The twisted shape of these curves clearly exhibits the role of the constant term $C_{x,y}$.

Fig. 4 shows the calculated on-axis spectrum in the vicinity of the fundamental harmonic (4.385 eV) for the case of measured magnetic field and for ideal (pure sinusoidal) helical field for the zero emittance electron beam. Fig. 5 shows the horizontal distribution of the fundamental for measured and sinusoidal magnetic fields.

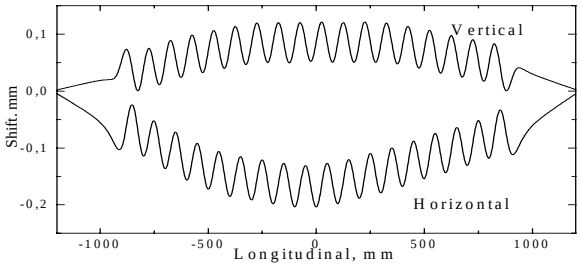

Fig. 3. Horizontal and vertical trajectories of the electron.

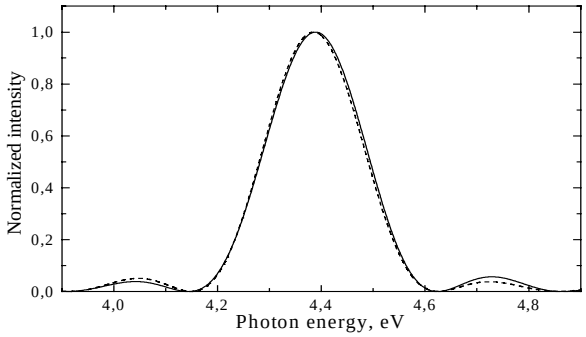

Fig.4. Computed on-axis brightness of the fundamental for the measured magnetic field (solid line) and for sinusoidal field (dashed line)

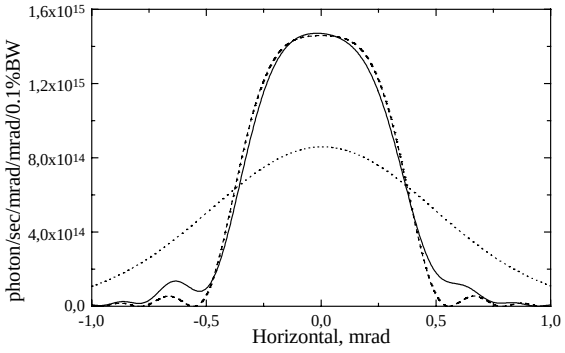

Fig. 5. Computed horizontal distribution of fundamental: measured field and zero emittance beam (solid curve),

measured field and real emittance beam (dotted curve), sinusoidal field and zero emittance beam (dashed curve).

Presented above results clearly demonstrate that the effect of magnetic field errors on the fundamental (which only will be used at helical mode) is negligible.

3.2 Linear mode

In the ideal case the magnetic field of any linear undulator has only one component (usually, vertical). But because of the complex arrangement of helical/linear undulator, its magnetic field contains both leading vertical magnetic field and slight horizontal field also, see Fig. 6. This horizontal component will shift the electron beam in vertical direction, see Fig 7. Electron beam has at the exit of undulator: horizontal deflection = 0.43 mrad, vertical deflection = -0.72 mrad.

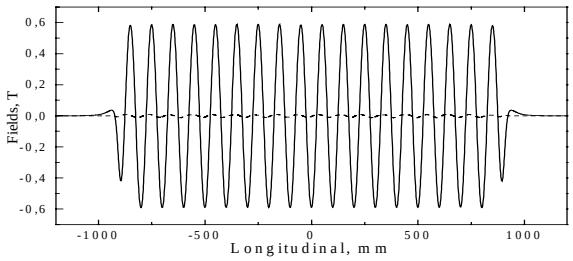

Fig. 6. Measured magnetic fields of helical/linear undulator at linear mode, gap=30 mm: vertical field (solid curve) and horizontal field (dashed curve).

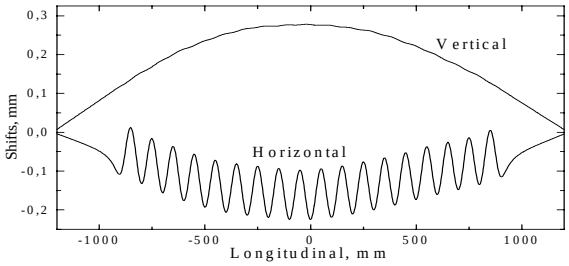

Fig. 7. Horizontal and vertical trajectories of the electron.

Again, let us consider the electromagnetic radiation properties that is our principal interest. Fig. 8 shows the on-axis spectrum (1st, 3rd, 5th, 7th and 9th harmonics) in the case of ideal magnetic field: sinusoidal vertical field and zero horizontal one. It is naturally that only the odd harmonics are generated by this magnetic field. The harmonic intensities increase with their number increase, because the deflection parameter is sufficiently large (5.6). Fig 9 shows the the on-axis spectrum in the case of measured magnetic field. From this figure we notice that the even harmonics are generated along the axis in the real case. The effect of higher harmonics degradation is clearly visible. But the shape and amplitude of the first harmonic are almost the some for both cases.

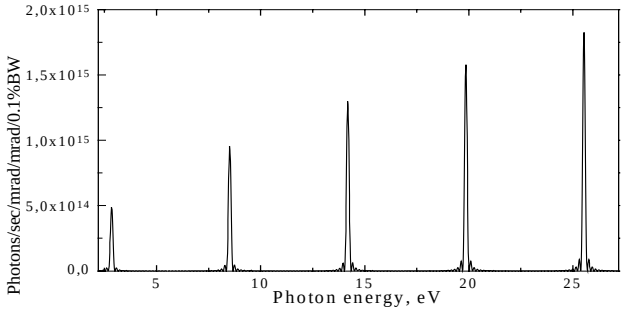

Fig. 8. On-axis spectrum in ideal planar magnetic field.

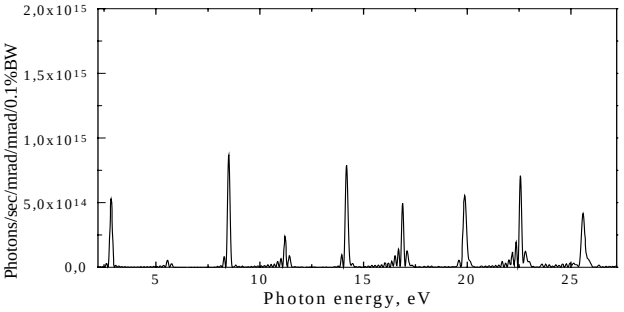

Fig. 9. On-axis spectrum in measured magnetic field.

4 REFERENCES

[1] M. Taniguchi and J. Ghijsen, J. Synchr. Rad., 5(3) (1998), p. 1176.

[2] A. Hiraya, K. Yoshida, S. Yagi, M. Taniguchi, S. Kimura, H. Hama, T. Takayama and D. Amano, J. Synchr. Rad., 5(3) (1998), p. 454.

[3] B. Kincaid, Nucl. Instr. and Meth., A246 (1986), p. 109.

[4] E.E. Alp and P.J. Viccaro, Nucl. Instr. and Meth., A266 (1988), p. 116.

[5] B. Kincaid, Nucl. Instr. and Meth., A291 (1990), p. 363.

[6] R. Carr, Rev. Sci. Instrum. 63(7) (1992), p. 3564.

[7] B.L. Bobbs, G. Rakowsky, P. Kennedy, R.A. Cover and D. Slater, Nucl. Instr. and Meth., A296 (1990), p. 574.

[8] R.P. Walker, Nucl. Instr. and Meth., A335 (1993), p. 328.

[9] Y. M. Nikitina, J. Pfluger, Nucl. Instr. and Meth., A359 (1995), p. 89.

[10] S. Sasaki, N. Matsuki, T. Takada, Rev. Sci. Instrum. 63(1) (1992), p. 409.

[11] R. Dejus, I. Vasserman, E.R. Moog and E. Gluskin, Rev. Sci. Instrum. 66(2) (1995), p. 1875.